ATMOSPHERIC TURBULENCE MEASUREMENTS AT MOUNT WILSON OBSERVATORY

NICHOLAS SHORT, WALT FITELSON, AND CHARLES H. TOWNES
Space Sciences Laboratory, University of California, Grizzly Peak at Centennial Drive, Berkeley, CA 94720

ABSTRACT

Simultaneous measurements of atmospheric temperature fluctuations at various altitudes and locations at Mount Wilson Observatory provide a quantitative description of local turbulence characteristics. The average rms value of the temperature fluctuations at an altitude of 150 feet is found to be 26% of the rms value at 9 feet, showing a substantial decrease with altitude for temperature fluctuations close to the ground. These rms values are found to be more heavily dependent on wind speed than on time of night, in contrast to prior belief. For measurements made close to the ground, the power spectra of the temperature fluctuations closely fit the Kolmogorov-Taylor prediction of -1.67 at frequencies up to 8 Hz, although at higher elevations some discrepancy is observed: the mean slope at 70 feet is approximately -1.50. The average size of major turbulent eddies is found to depend on wind speed, varying approximately linearly from about 1 to 25 m in both the horizontal and vertical directions for wind speeds between 0 and 8 m s^{-1}. Analysis of the correlation between horizontally separated sensors indicates that Taylor's approximation remains useful on timescales of 10–15 s, after which time the turbulence changes. This suggests that local measurements of temperature fluctuations could provide some appreciable correction to variations in path length in interferometric observations of stars caused by atmospheric turbulence.

Subject headings: atmospheric effects — techniques: interferometric — turbulence

1. INSTRUMENTATION

Because fluctuations in atmospheric temperature are closely related to fluctuations in index of refraction (under the assumption of constant pressure), precise temperature measurements at various times and spatial locations can provide useful information about the nature of atmospheric turbulence. To study the atmosphere in this manner, the Infrared Spatial Interferometer (ISI) group, located at Mount Wilson Observatory (MWO), has constructed a system capable of making temperature measurements at speeds of 22 Hz at two or more locations and at various elevations up to 70 feet.

The main components of this system are as follows: two telescoping masts, each mounted with five type E, style 2 thermocouples (Omega company model CO2-E) and a wind anemometer; two Campbell CR10X data units used to sample the thermocouples and the wind sensor; and a PC, used to collect the sampled data from the Campbell units. When completely raised, each mast had thermal sensors situated at approximately 9, 24, 39, 54, and 70 feet, giving temperature readings every 15 feet within the first 70 feet of the atmosphere. The wind anemometer was installed at the top of the mast (at 70 feet).

In addition, two sensors were mounted on top of the 150-Foot Solar Tower at MWO, providing two additional measurements at this altitude when desired. In the following discussions, the sensors are referred to by number instead of elevation, as listed in Table 1. Sensor 1 refers to the lowest mast thermocouple, located at 9 feet, and sensor 5 the uppermost mast thermocouple, located at 70 feet. Sensors 6 and 7 refer to the two solar tower sensors, which are still more elevated.

The results of 500 s of a typical temperature reading by one of our sensors is shown in Figure 1.

2. POWER SPECTRA OF TEMPERATURE MEASUREMENTS

According to the theory of atmospheric turbulence commonly known as Kolmogorov theory, the logarithmic power spectrum of fluctuations in certain atmospheric parameters, such as the index of refraction or temperature, should exhibit a power-law dependence on frequency, ν^{β}. While this theory typically applies to spatial power spectra, it can be extended to the time domain through use of the Taylor approximation, which assumes the fluctuations are "frozen" in the atmosphere and are blown past any specific point with a wind of constant velocity V. Under this approximation, temporal power spectra should exhibit similar power-law behavior. For measurements taken at a point source, the theory predicts $\beta = -5/3$ for temporal frequencies above $\nu = V/L_{K}$, where L_{K} is the outer scale of turbulence, or the spatial scale on which the assumptions of Kolmogorov theory become inaccurate or nonapplicable.

Discrepancies between the power spectra of real measurements and theoretical predictions can have important implications for the potential performance of existing telescopes at astronomical observation sites. The fitting procedure used to determine the power spectrum slopes of the present measurements is discussed in § 2.1, while trends observed in the average spectrum slopes, as well as any discrepancies from theoretical predictions, are presented in § 2.2.

2.1. *Fitting Procedure*

A typical power spectrum, taken from a 25 minute set of temperature fluctuations, is shown in Figure 2. The average wind speed during this particular data set was 3.90 m s^{-1}.

To determine the slope of each individual spectrum, data for frequencies lower than 0.1 Hz were discarded, and the

TABLE 1

SENSOR NUMBERS AND
CORRESPONDING
ELEVATION

Sensor Number	Elevation (feet)
1................................	9
2................................	24
3................................	39
4................................	54
5................................	70
6................................	154
7................................	158

NOTE.—Each of two movable masts contained sensors numbered 1–5, while sensors 6 and 7 were mounted on top of the 150-Foot Solar Tower telescope.

FIG. 2.—Typical logarithmic power spectrum (PSD 2002 July 25; mast 1, set 1, sensor 5). The spectrum is averaged in this case so the points appear equally spaced when plotted logarithmically. This type of averaging is used here for visual presentation only and was not used when fitting the spectra. The exceptionally high point at about 10 Hz is evidence of unwanted pickup of an external signal.

data for frequencies between 0.1 and 8.0 Hz were fit to a three-parameter model of the form

$$P = a + b\frac{\nu^{-\beta}}{1 + (2\pi\nu\tau)^2} \qquad (1)$$

where P represents the power, ν the temporal frequency, and τ the time constant of the response of the temperature detector. In this model, a and b are constants, with a representing the value of the noise floor in squared degrees per hertz; and β represents the value of the slope of the logarithmic power spectrum.

The denominator in equation (1) is a correction for the time constant response of the thermocouples, with τ representing the value of the time constant in seconds. The effect of the time constant is visible in Figure 2 as a slight "knee" in the spectrum, or a slight reduction in power at frequencies above 1 Hz. Testing of the system showed this effect to be due to the time constant response of the thermocouples, which was measured to vary between 150 and 65 ms, depending on the wind speed (the thermocouples reacted more slowly at slower wind speeds). The value of τ used in the fitting procedure for all data was determined from a model that describes the time constant response of the
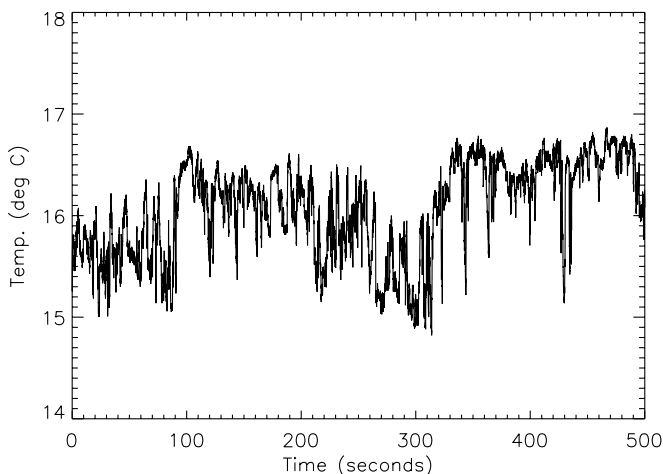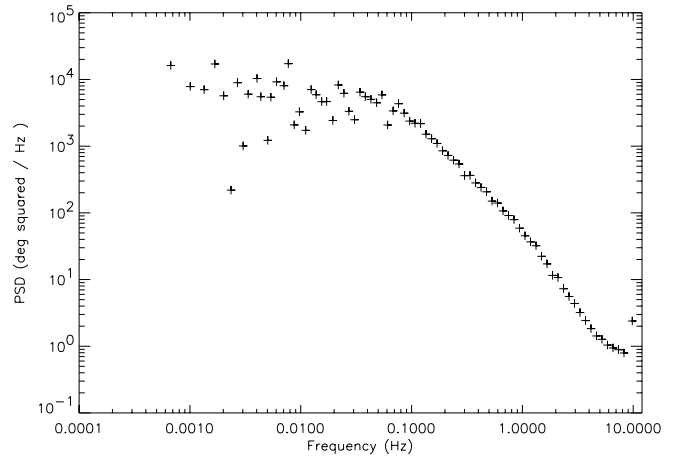
thermocouples as a function of wind speed: $\tau = c/(d + V)$, where V represents the wind speed, and the constants c and d were derived from laboratory tests to be 0.685 m and 4.71 m s^{-1}, respectively.

Before the spectra were fit, they were averaged slightly to reduce the computation time, each point in the fitted curves representing the average of 30 points from the original spectrum. For each fit, the three parameters a, b, and β of equation (1) were allowed to vary randomly, and the best fit was chosen as the one that produced the smallest χ^2, where

$$\chi^2 = \sum_{i=0}^{N-1} \frac{(P_i - P_{\mathrm{fit},i})^2}{\sigma_i^2} \qquad (2)$$

and each σ_i represents the standard deviation associated with each point P_i.

Once the fitting procedure was run on each individual spectrum, the average values of the slopes (the value β in eq. [1]) were tabulated for each sensor, with various average wind speeds over the course of the data sets, in order to get a statistical sense of how these spectral slopes vary with altitude and wind speed. Some fits were not included in this tabulation, namely those fits that returned an excessively high value for the noise floor (the constant a in eq. [1]), most likely because of high-frequency pickup; and those that had an abnormally large χ^2 minimum value, indicating the data could not be well fitted to the model. Table 2 shows the results of this tabulation. Note that the values of β are tabulated, and so the numbers are positive although they indicate a negative slope in the fit.

2.2. Trends in Spectrum Slopes

Two trends are noteworthy in Table 2. First, at any given altitude the average value of β stays relatively constant with increasing wind speed.[1] However, for any given range of wind speeds, the average value of β clearly does decrease (so

FIG. 1.—Typical temperature reading from May 15, sensor 3. The graph shows 500 s of data collected at an elevation of 70 feet.

---

[1] The numbers in the table can be slightly misleading at low wind speeds because there is large scatter in the slope values at wind speeds below 2 m s^{-1}, with a few abnormally small values of β biasing the overall average.

TABLE 2
POWER SPECTRUM SLOPES

WIND SPEED (m s^{-1})	SLOPE				
	Sensor 1	Sensor 2	Sensor 3	Sensor 4	Sensor 5
0–1	1.73 (34)	1.70 (3)	1.40 (33)	1.40 (36)	1.28 (35)
1–2	1.76 (63)	1.66 (49)	1.56 (61)	1.35 (57)	1.36 (56)
2–3	1.76 (47)	1.68 (39)	1.59 (45)	1.49 (43)	1.48 (42)
3–4	1.84 (18)	1.83 (15)	1.69 (19)	1.64 (18)	1.59 (19)
4–5	1.74 (34)	1.68 (25)	1.62 (32)	1.56 (29)	1.58 (31)
5–6	1.65 (21)	1.67 (17)	1.62 (21)	1.53 (18)	1.60 (20)
6–7	1.61 (10)	1.61 (7)	1.59 (8)	1.56 (7)	1.56 (9)
7–8	1.71 (2)	1.70 (2)	1.64 (2)	1.49 (2)	1.64 (2)

NOTES.—The slopes are tabulated as a function of average wind speed for each sensor. Sensors 1–5 are at elevations of 9, 24, 39, 54, and 70 feet, respectively. The numbers in parentheses indicate the number of data sets averaged. Note that the values of β are tabulated and so are positive, although the positive numbers indicate a negative slope in the fit.

the average spectrum slope becomes less negative, or more shallow) with increasing altitude. For example, at wind speeds between 2 and 3 m s^{-1}, the slope parameter β decreases from 1.76 to 1.48 between sensor 1 (9 feet elevation) and sensor 5 (70 feet).

Averaging over all the data sets at a given elevation, the mean value of β is 1.73, 1.69, 1.59, 1.50, and 1.51 for sensors 1–5, respectively. The slope parameter β takes on values larger than the Kolmogorov-Taylor (KT) value of 1.67 at the lowest altitudes, perhaps because KT theory assumes no boundary conditions, an assumption that is violated near the ground. Slopes more shallow than 1.67 are observed at higher elevations and greater wind speeds and may correspond to previously reported slopes smaller than KT expectations (Bester et al. 1992; Buscher et al. 1995; Linfield, Colavita, & Lane 2001).

Although this type of analysis does not provide a precise determination of the value of the outer scale, it can be roughly estimated from visual inspection of spectra like the one shown in Figure 2. The turning point in this spectra appears to lie at 0.1 Hz, which for a wind speed of 3.90 m s^{-1} suggests an outer scale of approximately 40 m.

3. ROOT MEAN SQUARE VALUES OF THE TEMPERATURE FLUCTUATIONS

While it is commonly known that a substantial fraction of the atmospheric turbulence occurs at low altitudes, it is also useful to have a more quantitative idea of how rapidly the turbulent fluctuations decrease with increasing altitude. Any possible dependency of the magnitude of turbulent fluctuations on time of night and wind speed is also of interest. Analysis of the rms values of the temperature fluctuations was performed as follows.

For each set of temperature readings, a running mean (or boxcar average) of a 60 s width was subtracted to remove the long-timescale, low-frequency variations, since temperature changes over such long time periods probably do not represent the random turbulence described by KT theory.[2] The data sets were then broken into 5 minute segments, and

the rms value of the temperature fluctuations in degrees Celsius for each segment was tabulated as a function of (1) average wind speed during the course of the data set, and (2) the relative time of night.[3] See Tables 3 and 4 for tabulations of these values. In both tables, the numbers in parentheses indicate the number of 5 minute data sets that were averaged to produce the mean value shown.

The rms values tend to increase with increasing wind speed at a given elevation, somewhat as expected. For example, the average rms values for sensor 7 increase from 0.03 to 0.16, a factor of 5.3, as the wind increases from 0.5 to 3.5 m s^{-1}. In addition, averaging all of the data at each given elevation, the mean rms value decreases from 0.29°C at an elevation of 9 feet, to 0.15°C at an elevation of 70 feet, and to 0.075°C at an elevation of 150 feet (sensors 6 and 7 were averaged together since they are less than 2 feet apart). Thus, the mean rms magnitude of the temperature fluctuations at an altitude of 70 feet is 52% of the mean rms value at an altitude of only 9 feet, and the mean rms value at 150 feet is roughly 26% of the value at 9 feet. At low wind speeds, the difference in the magnitude of the fluctuations with altitude is even larger.

The data presented in Table 4 show changes in the rms values with respect to the relative time of night. It has often been hypothesized that sunrise and sunset (0 and 1 on the relative timescale) offer the best possible seeing conditions, since the ground temperature is closest to the air temperature at these times, and hence the magnitude of fluctuations caused by convection and other turbulent processes is subsequently minimized. Measurements of the refractive index structure parameter C_n^2, such as those presented in Lawrence (1976), lend credibility to this hypothesis.[4] For present measurements, this phenomenon should be reflected in smaller average rms values at these times. However, the averaged values presented in Table 4 do not show any drastic changes close to sunrise and sunset. This indicates

---

[2] In addition, fluctuations in these timescales do not substantially contribute to distortions in phase or path length in interferometric observation of starlight at infrared and optical wavelengths.

[3] Relative time of night refers to a fractional timescale from sunset (a value of 0) to sunrise (a value of 1). Mathematically, the relative time of the data set is the time after sunset divided by the total time from sunset to sunrise.

[4] These measurements were made using fine-wire resistance thermometers 2 m above the ground and are somewhat similar to the measurements discussed in this paper.

TABLE 3

Root Mean Square Values as a Function of Wind Speed for Data Taken with Sensors on the Masts and on the Solar Tower

Wind Speed (m s^{-1})	Root Mean Square Value						
	Sensor 1	Sensor 2	Sensor 3	Sensor 4	Sensor 5	Sensor 6	Sensor 7
0.0–1.0	0.25 (8)	0.19 (8)	0.10 (8)	0.09 (8)	0.06 (8)	0.02 (7)	0.03 (8)
1.0–2.0	0.29 (101)	0.23 (101)	0.19 (101)	0.12 (101)	0.08 (101)	0.03 (86)	0.03 (101)
2.0–3.0	0.33 (19)	0.27 (20)	0.21 (20)	0.15 (20)	0.12 (20)	0.04 (15)	0.05 (20)
3.0–4.0	0.23 (16)	0.30 (33)	0.29 (33)	0.26 (33)	0.22 (33)	0.15 (14)	0.16 (33)
4.0–5.0	0.28 (24)	0.27 (35)	0.25 (35)	0.21 (35)	0.20 (35)	0.12 (14)	0.15 (35)
5.0–6.0	0.29 (20)	0.24 (35)	0.26 (35)	0.25 (35)	0.23 (35)	0.11 (8)	0.18 (35)
6.0–7.0	0.29 (8)	0.26 (9)	0.24 (9)	0.20 (9)	0.17 (9)	0.11 (1)	0.09 (9)

Notes.—The rms values are tabulated according to average wind speed. The data presented here were taken from five different nights in which data from one mast were gathered simultaneously with two sensors (6 and 7) mounted on top of the 150-Foot Solar Tower. The rms values are obtained from 5 minute segments of data after subtraction of a running mean, and the numbers in parentheses show the total number of sets averaged. Sensors 1–5 are at elevations of 9, 24, 39, 54, and 70 feet, respectively.

that while there may be variations with time for an individual day or night, the rms value of the temperature fluctuations is statistically more dependent on overall wind speed than on time.

4. CORRELATION ANALYSIS

Additional information about the nature and behavior of the atmosphere can be obtained through an analysis of the correlation between two sensors separated by some distance. Specifically, correlation analysis between different sensors can show how the fluctuations move about, or translate, temporally in both the horizontal and vertical directions and can provide an estimate of the average spatial dimensions of the major turbulent eddies.

The general method used in computing the correlations is as follows: For all correlations considered in this paper, a running mean (or boxcar average) of a 30 s width was subtracted from each temperature reading prior to the correlation calculation. The correlation coefficient between individual data sets of 10 minute lengths was then computed out to ±100 s on a delayed time axis. For each correlation curve, the following was then recorded: the average wind speed and direction for the data set concerned, the peak value of the correlation coefficient, the lag or delayed time

value at which the correlation curve peaks, and the width of the correlation peak at half-maximum.

As a simple example of correlation, Figure 3 shows the observed time delay for correlations between two temperature sensors on the same mast, one sensor 9 feet above the other. It might be expected that for a perfectly horizontal wind the time delay between the two sensors would be essentially zero, which it is in Figure 3 for the higher wind speeds. The small but increasingly negative delays at lower wind speeds may be related to some slowing of the wind for positions closer to the ground, if wind speed gradients have the effect of "tilting" or "elongating" the shape of the predominant eddies. At very low wind speeds, the correlations are quite scattered, reflecting the fact that at these speeds the extent or size of the major turbulence decreases, as is demonstrated below. If at low overall wind speeds the average size of the turbulent eddies is smaller than the separation of the sensors, then the correlation between sensors should be weak and the delay values more randomly scattered.

4.1. Horizontal Correlations and Taylor's Approximation

The correlation between sensors separated horizontally (parallel to the ground) can provide a test of Taylor's hypothesis, since the wind is assumed to have a negligible vertical component and can, depending on the conditions,

TABLE 4

Root Mean Square Values as a Function of Time of Night for Data Taken with Sensors on the Masts and on the Solar Tower.

Time	Root Mean Square Value						
	1	2	3	4	5	6	7
0.0–0.1	0.30 (11)	0.26 (13)	0.27 (13)	0.18 (13)	0.10 (13)	0.06 (4)	0.06 (13)
0.1–0.2	0.20 (29)	0.26 (36)	0.25 (36)	0.20 (36)	0.14 (36)	0.04 (20)	0.07 (36)
0.2–0.3	0.30 (29)	0.29 (38)	0.25 (38)	0.20 (38)	0.18 (38)	0.07 (19)	0.09 (38)
0.3–0.4	0.26 (38)	0.25 (38)	0.22 (38)	0.16 (38)	0.12 (38)	0.08 (28)	0.08 (38)
0.4–0.5	0.33 (32)	0.25 (41)	0.24 (41)	0.18 (41)	0.14 (41)	0.06 (24)	0.11 (41)
0.5–0.6	0.27 (17)	0.23 (28)	0.20 (28)	0.18 (28)	0.16 (28)	0.06 (17)	0.14 (28)
0.6–0.7	0.30 (19)	0.21 (26)	0.17 (26)	0.19 (26)	0.18 (26)	0.04 (19)	0.12 (26)
0.7–0.8	0.42 (6)	0.23 (6)	0.16 (6)	0.20 (6)	0.15 (6)	0.02 (6)	0.03 (6)
0.8–0.9	0.41 (7)	0.39 (7)	0.22 (7)	0.15 (7)	0.23 (7)	0.04 (7)	0.04 (7)

Notes.—Tabulation of rms temperature values according to relative time of night. Relative time is a fractional timescale in which a value of 0 corresponds to sunset, and a value of 1 to sunrise.
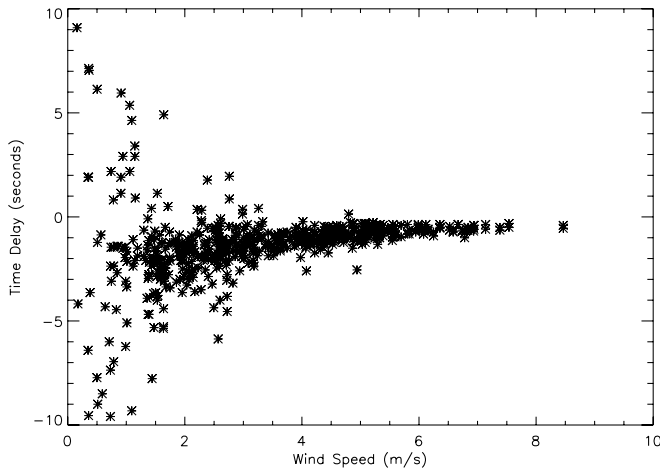
Fig. 3.—Observed time delay for correlations between sensors 4 and 5, separated by 9 feet in height, on each mast. The scattering of time delay values at low wind speeds may indicate a dependence of spatial size on wind speed, which is in fact demonstrated by other measurements.

be blowing in the direction of separation of the sensors. Recall that the Taylor approximation assumes temperature fluctuations are " frozen " in the atmosphere and are blown from one point to another by a wind of constant velocity V.

If Taylor's hypothesis is valid, then in the special case in which the wind is blowing in the direction of separation of the sensors, the observed time delays should match closely with the values estimated from the wind speed measurements. Figure 4 compares these values for correlations between sensor 5 on both masts, and for sensor 2 on both masts. In the data presented here, the wind was blowing at least 93% in the direction of separation of the masts (or, in terms of degrees, within 22° of the direction of separation on average), and the solid lines in both panels represent the value of the estimated time delay, defined as the horizontal separation in meters divided by the component of the wind speed in the direction of the separation in meters per second. As is apparent, the observed delays agree fairly well with the estimated values, with several data sets showing good correlation out to time delays of 14–15 s for sensor 5. The time

delay values observed for sensor 2 are generally larger in magnitude than those of sensor 5 and those calculated from wind speed, perhaps because of slower wind speeds closer to the ground.[5]

Another way of testing Taylor's hypothesis is to examine how the magnitude of correlation (the peak value of the correlation coefficient) changes with travel time in the air. Figure 5 shows the peak value of the correlation coefficient for correlations between sensor 5 on each mast and sensor 2 on each mast, plotted as a function of the estimated time delay. In the 15 nights of data analyzed in this section, the masts were separated by distances ranging from 0.3 to approximately 24.3 m. Both plots show only data in which the wind was blowing at least 93% in the direction of separation. The x-axis is plotted logarithmically, and so the roughly linear relationship in the plot suggests an approximately exponential decrease in the correlation coefficient as a function of time delay. For such a decay, of the form $e^{-t/\tau}$, a time constant τ of approximately 12 s fits the data and is not strongly dependent on height above the ground. If we assume that correlation coefficients below 0.2 do not represent significant correlation, then the two sensors at an elevation of 70 feet show significant correlation out to time delays of approximately 15 s, consistent with our previous analysis of the correlation time delays (Fig. 4). The two sensors at an elevation of 24 feet show similar results, although the magnitude of the correlations is generally somewhat smaller, and correlation decreases to 20% in a slightly shorter time.

That both of these representations (Figs. 4 and 5) are consistent is encouraging and indicates that Taylor's hypothesis has some validity on timescales as large as 10–15 s, with smaller timescales observed toward the ground, and slightly larger timescales at higher elevations. Since these timescales are not dependent on wind velocity, it follows that the spatial distances on which the Taylor approximation can be usefully applied are dependent on (and are approximately proportional to) wind speed.

---

[5] Recall that the estimated time delay is dependent on wind measurements made at the top of the mast, near sensor 5.
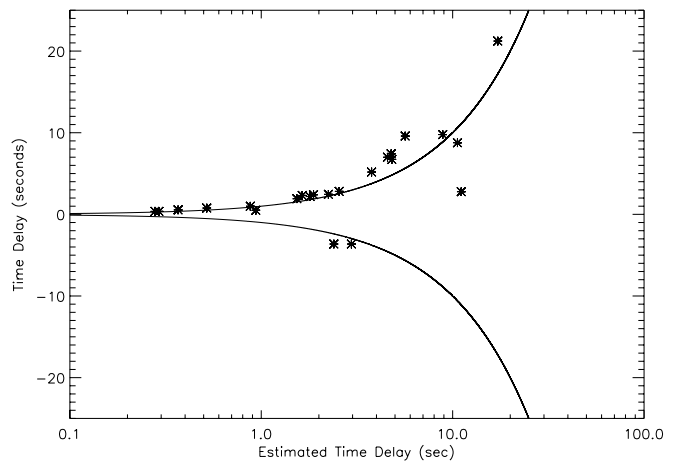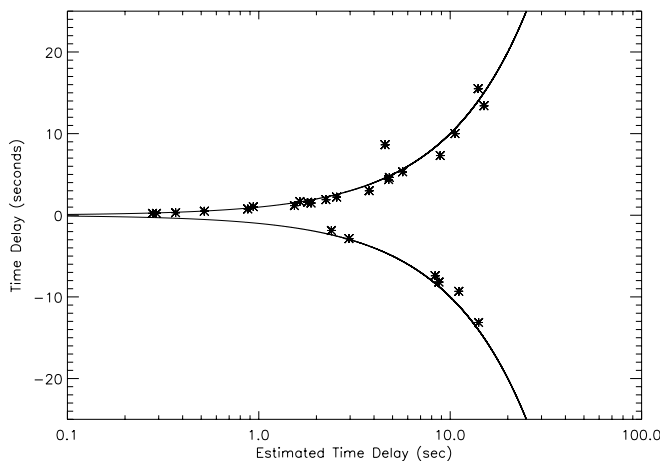

Fig. 4.—Observed time delay between masts for sensors 5 (*left*) and 2 (*right*) when the masts are separated by various distances. The wind was blowing at least 93% in the direction of separation of the sensors. The solid lines indicate the value of the estimated time delay derived from measurements of the wind speed and direction; the two lines in each figure correspond to opposite wind directions.
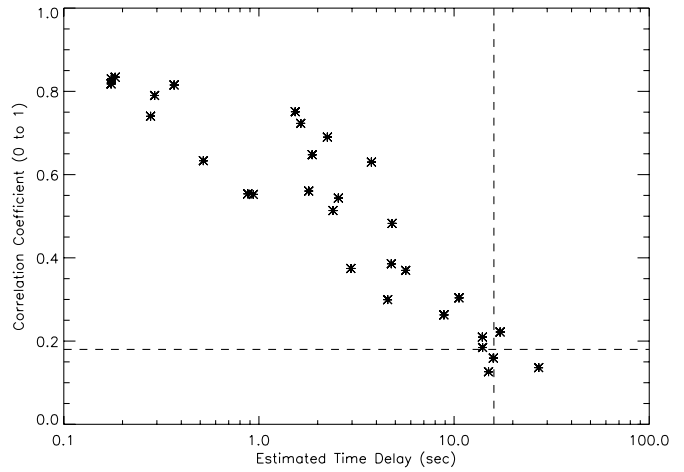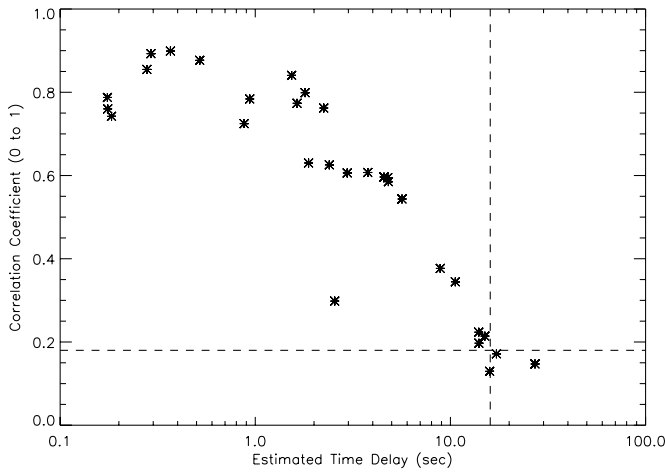
FIG. 5.—Peak values for correlations between two temperature sensors at the same elevation but on different masts separated in the direction of the wind by distances of 0.3–24 m. The data show the results for correlations between sensor 5 on each mast (*left*) and between sensor 2 on each mast (*right*), and show only those data sets collected when the wind was blowing at least 93% in the direction of separation of the sensors. The dotted lines are visual aides that approximate the time delay value at which the correlation coefficient values, on average, drop below 0.18. These plots indicate an exponential decay of correlation with a time constant of approximately 12 s.

4.2. Correlations Indicating the Geometrical Size of Major Fluctuations

In addition to testing Taylor's hypothesis, fluctuation correlations can also be used to approximate the geometrical size of the turbulent eddies, the subject of this section. Qualitatively, when the wind is blowing perpendicular to the separation of the sensors, the sensors should be well correlated at spatial separations on the order of or smaller than the average spatial size of the turbulent eddies. At spatial separations larger than the average size, the correlation should be rather poor.

Figure 6 shows the peak value of the correlation coefficients for correlations between sensors 4 and 5 on each mast and indicates that the peak value of the correlations at this vertical separation (15 feet) depends on the average value of the wind speed. Hence, the vertical size of the major fluctuations must likewise be dependent on wind speed.

Figure 7 indicates more explicitly how the size of major turbulence in the vertical direction varies with wind speed. Each symbol in the figure represents the average correlation coefficient at a given vertical separation and in a particular range of wind speeds. By focusing on any one range of wind speeds, the mean vertical spatial size of the turbulent eddies can be estimated by interpolating (or extrapolating, for the higher wind speeds) the point at which the peak value becomes insignificant, which for this data might be taken as a correlation coefficient value of 0.16, represented by the dashed line in the figure. For wind speed ranges of 7–8, 5–6, 3–4, and 1–2 m s^{-1}, the correlation coefficient drops to 0.16 at separations of approximately 28, 24, 19, and 11 m, respectively.

These approximate sizes are plotted as a function of wind speed in Figure 8 to visually, although not quantitatively,
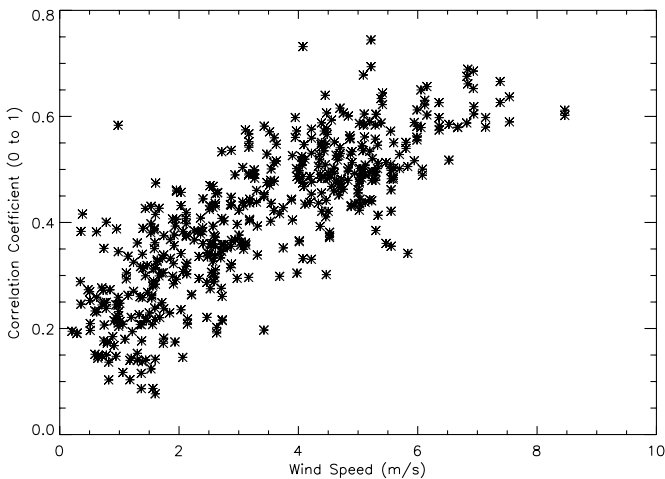

FIG. 6.—Peak value of the correlation coefficient for vertical correlations between sensors 4 and 5 on each mast. The peak values at this particular separation (15 feet) are dependent on wind speed, indicating that the average spatial size of the turbulent eddies in the vertical direction is likewise dependent on wind speed.
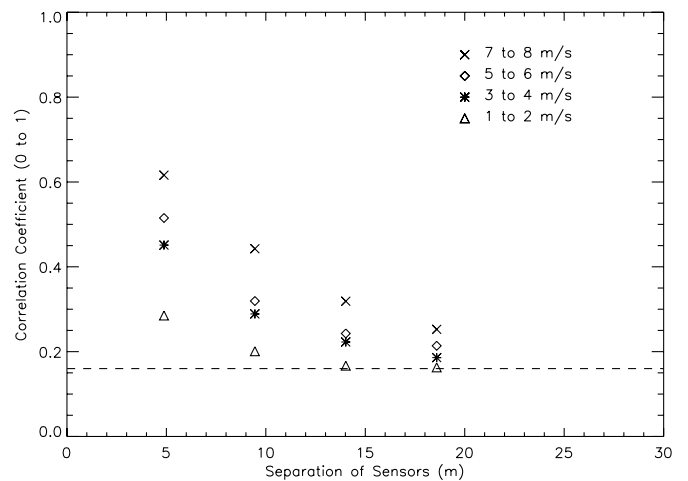

FIG. 7.—Peak value of the correlation coefficient as a function of the vertical separation of the sensors, for a variety of different wind speed ranges. The average vertical spatial size of the turbulent eddies can be estimated by interpolating or extrapolating the approximate point at which the correlation coefficients in a given range of wind speeds (like symbols) intersect the dashed line (a correlation coefficient of 0.16).
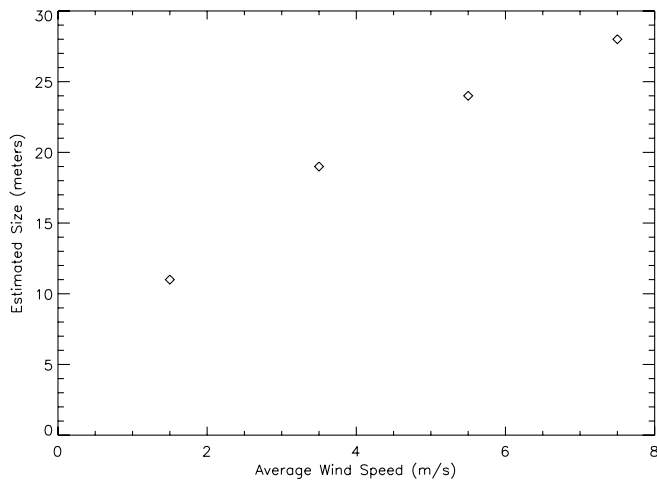
FIG. 8.—Estimated vertical scale size of the turbulent eddies and the dependence of this quantity on wind speed. The vertical sizes are estimated by eye from the data presented in Fig. 7 and are plotted here as a qualitative, not quantitative, illustration.

FIG. 10.—Average amount of correlation between sensor 5 on both masts (at 70 feet) for a variety of mast separations and wind speed ranges, with the wind direction at least 80% perpendicular to the direction of separation. Each wind speed range is designated by a particular symbol, with the corresponding range of speeds printed in the upper right-hand corner.

illustrate the variation of vertical scale sizes with wind velocity. As a rough approximation, if the vertical size is assumed to vary linearly between the points plotted, then the size of major turbulence in the vertical direction varies as $(2.8 \text{ s})V$, where V is the wind velocity in meters per second.

A similar type of analysis can be performed on data taken when the wind is blowing perpendicular to two sensors separated in the horizontal direction, or two sensors at the same elevation but on separate masts. Figure 9 shows the peak correlation values for correlations between sensor 5 on both masts when the masts were separated by approximately 4.8 m. The data are plotted as a function of average wind speed and show only the data sets in which the wind was blowing at least 80% perpendicular to the direction of separation of the sensors. The plot indicates that the peak value of the correlations at a given separation depends on the average value of the wind speed, much as in Figure 6 for vertical correlations.

Figure 10 presents the dependence of the average correlation magnitude both on horizontal separation and on average wind speed for correlations between sensor 5 on each mast (both at an elevation of 70 feet) when the wind was blowing in a direction at least 80% perpendicular to the separation. The figure shows the average of the correlation peak values at each of three separations (4.8, 12.8, and 24.3 m) for data taken in a variety of wind speed ranges. The dashed line in the plot indicates the value at which the correlation seems to become insignificant—at a correlation coefficient value of 0.22. Because of the scarcity of data in this analysis, it is difficult to interpolate and extrapolate approximate sizes as in Figure 7 for most wind speed ranges, the best case being for speeds between 4 and 5 m s^{-1}, which indicates an average size of approximately 15 m. However, we can use the data available to conclude that the horizontal spatial extent of the major turbulence perpendicular to the wind velocity exhibits a dependence on wind speed similar to that observed for vertical separations.

The average horizontal size in the direction of the wind can be estimated from an autocorrelation curve by multiplying the half-width of the autocorrelation peak, in seconds, by the average wind speed, in meters per second. Figure 11 shows the resulting average spatial sizes for all of the temperature readings for sensor 5 (*left*) on both masts and for sensor 3 (*right*) on both masts. The figure demonstrates that the average horizontal size in the direction of the wind also varies approximately linearly with wind speed.

Figures 7 and 8 show that the vertical size of the turbulent eddies varies with wind velocity V roughly as $(2.8 \text{ s})V$ for velocities between 1 and 8 m s^{-1}. Figure 11 shows that horizontal size variations in the direction of the wind are approximately the same, perhaps $(2.2 \text{ s})V$, and Figure 10, although more limited in data, indicates similar size variations in the direction perpendicular to the wind. Thus, even near the ground, the turbulence fits Kolmogorov's assumption of isotropy reasonably well.

Figure 5 shows an exponential decay time for major turbulent eddies, with a time constant of about 12 s. Thus,
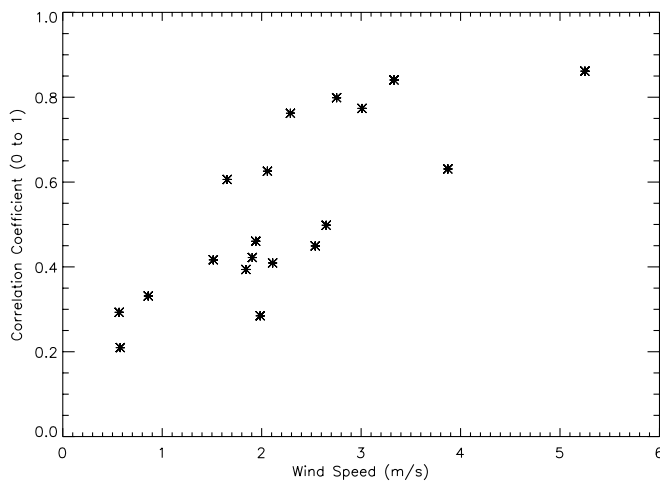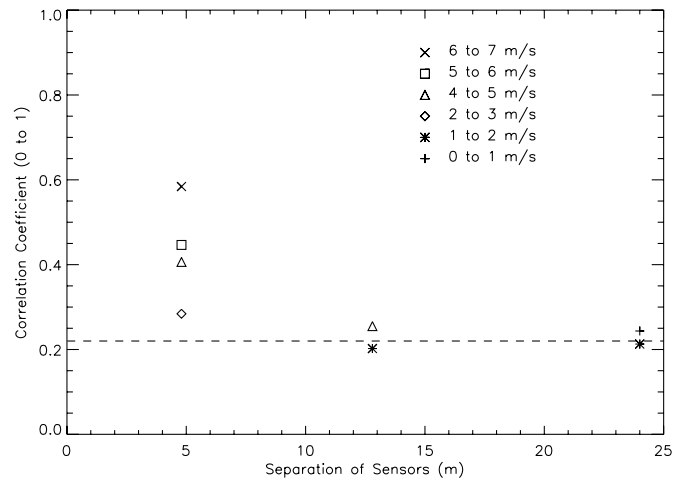

FIG. 9.—Peak values for correlations between sensor 5 on each mast when the masts are separated by 4.8 m and winds are approximately perpendicular to the direction between the masts. The peak values are plotted as a function of average wind speed during the course of the data correlated.
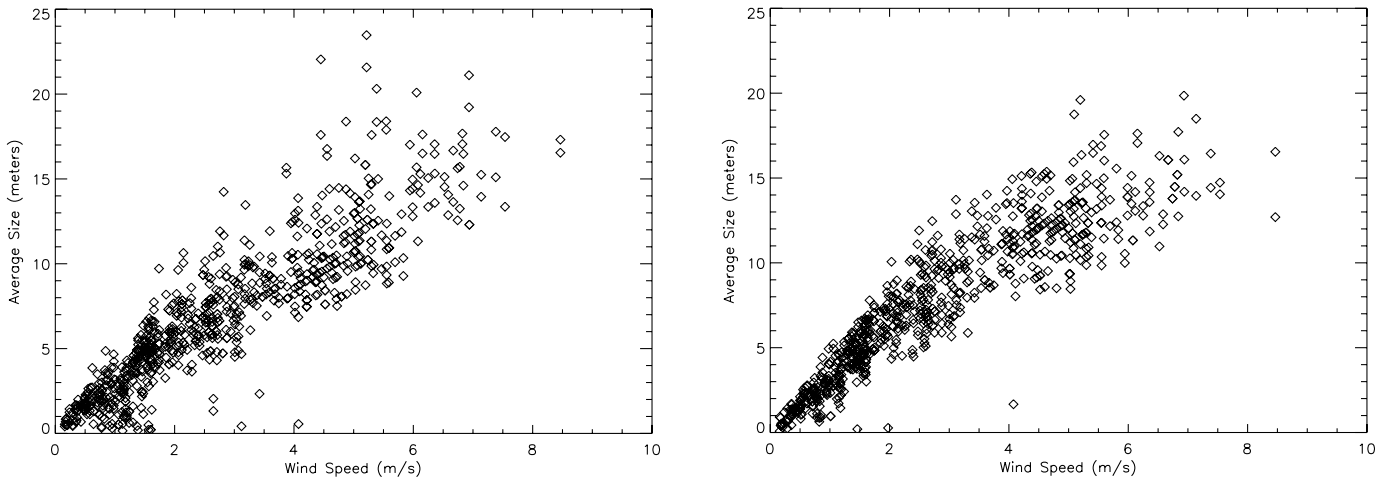
FIG. 11.—Average size of the turbulence eddies plotted as a function of average wind speed. The average size was obtained by multiplying the half-width of the autocorrelation curve (in seconds) for a given temperature reading by the average wind speed (in meters per second). This figure shows the results for sensors 5 (*left*) and 3 (*right*) on both masts at elevations of 70 and 39 feet, respectively.

one can conclude that turbulence of size $2.5V$ moves past a sensor a distance of $12V$, which is substantially larger than its size, before it undergoes any major change. Another way of saying this is that the translation time (the time it takes for an entire turbulent eddy to travel or translate an appreciable distance in the atmosphere) is shorter than the evolution time (the time it takes for the turbulence to evolve through random processes into some different form).

5. CONCLUSION AND COMPARISON WITH OTHER RESULTS

Simultaneous measurements of turbulence at a number of points within 150 feet of ground level at Mount Wilson Observatory show that the Kolmogorov-Taylor model of atmospheric turbulence is a reasonable approximation, although measured deviations from it are of importance. For measurements made at a point source, the KT model predicts a power spectrum of fluctuations proportional to $\nu^{-5/3}$ for the higher frequencies, and a spectrum power independent of frequency at low frequencies because of an outer scale of turbulence.

At very low altitudes, the power spectrum of temporal fluctuations in air density is found to vary somewhat more rapidly with frequency than predicted by the KT model, and at higher altitudes somewhat more slowly than predicted. For example, averaging over all wind speeds, the mean logarithmic slopes of the power spectra are 1.73, 1.69, 1.59, 1.50, and 1.51 for altitudes of 9, 24, 39, 54, and 70 feet, respectively, as compared to the KT model values of 5/3, or 1.67. Slopes smaller than predicted by the KT model have also been reported by other observers (Bester et al. 1992; Buscher et al. 1995; Linfield et al. 2001). However, it is important to note that measurements made in this study, which rely on point-source temperature measurements within the first 150 feet of the atmosphere, are substantially different from these previous measurements, which rely on observations of starlight that has propagated through the entire atmosphere, or on measurements of path length fluctuations in optical interferometers near the Earth's surface.

The maximum size of major turbulence is found to vary substantially with wind speed, being approximately propor-

tional to it for normal wind speeds. This striking dependence of turbulence size on wind speed has previously received little attention. At wind speeds in the range of 2–8 m s^{-1}, the major turbulence size is approximately $(2.5\ \mathrm{s})V$, where V is the wind speed in meters per second. The size of major turbulence is thus usually in the range of 5–30 m, depending on wind speed. This makes the frequency close to constant, i.e., approximately 0.1 Hz, at which point the slope of the spectral power becomes less steep because of the outer scale of turbulence. The " outer scale " itself is comparable but is slightly larger than this size of 5–30 m, perhaps by a factor of 2. Although dependence on wind speed has not been previously noted, the outer scales found are reasonably consistent with those that others have reported. At the Palomar Testbed Interferometer, outer scales of 10–25 m were found (Linfield et al. 2001), with no specified wind speeds, although the speed was said to be generally less than 4 m s^{-1}. Measurements at the William Herschel Telescope in La Palma yielded outer scales of only 2 m with wind speeds estimated at 10 m s^{-1} (Nightingale & Buscher 1991). However, this result does not seem very secure, because it involves a limited number of measurements with baselines no longer than 2 m.

The size of major turbulence is shown to be approximately the same in the horizontal and vertical directions. Such determinations have apparently not received much attention, although a brief discussion can be found in Wheelon (2001, p. 47). This confirms the isotropy assumed by Kolmogorov.

The Taylor approximation of " frozen " turbulence clearly only applies over a limited time, since turbulent eddies develop and change over time. The time for major turbulence changes has been measured to be in the range of 10–15 s. Hence, the distances over which the Taylor approximation applies are typically in the range of 10–100 m, depending on wind speed. These are the distances for which a measurement of turbulence at one position can provide useful prediction of turbulence downwind.

Near the ground, turbulence is found to decrease substantially in magnitude with increasing altitude. For altitudes of 9, 70, and 150 feet, the relative magnitude of turbulence was found to be 1, 0.52, and 0.26, respectively. Such effects have

been noted previously, particularly by Treuhaft et al. (1995), who described turbulence as associated with two atmospheric layers, the first extending to about 45 m and contributing as much as one-half the total seeing problem of the entire atmosphere. The present measurements find a continuous decrease in magnitude of turbulence up to a height of about 50 m, with no measurements available at higher altitudes.

On the basis of the present results, it appears practical to obtain useful corrections for perhaps one-third of the path-length fluctuations through the atmosphere by making adequate measurements near the ground, either upwind or downwind from the path of observations. The precise amount of correction cannot be predicted, because a quantitative measurement of path length fluctuations in the upper atmosphere compared to the lower atmosphere has not yet been made known. Measurements for such corrections can appropriately be made up to an altitude of 70 feet or more and should preferably be quite near the line of sight and in the direction of the wind. The ISI is well equipped to make these types of measurements, and future work may examine the usefulness of this method for correction in interferometric observations. An alternative possibility for interferometry refinement, which uses light scattering to measure atmospheric densities, has also been suggested (Townes 2002).

REFERENCES

Bester, M., Danchi, W. C., Degiacomi, C. G., Greenhill, L. J., & Townes, C. H. 1992, ApJ, 392, 357
Buscher, D. F., et al. 1995, Appl. Opt., 34, 1081
Lawrence, R. S. 1976, Proc. SPIE, 75, 2
Linfield, R. P., Colavita, M. M., & Lane, B. F. 2001, ApJ, 554, 505
Nightingale, N. S., & Buscher, D. F. 1991, MNRAS, 251, 155
Townes, C. H. 2002, ApJ, 565, 1376
Treuhaft, R. N., Lowe, S. T., Bester, M., Danchi, W. C., & Townes, C. 1995, ApJ, 453, 522
Wheelon, A. D. 2001, Electromagnetic Scintillation. I. Geometrical Optics (Cambridge: Cambridge Univ. Press)